CHAPTER 17

COLLOIDAL SEMICONDUCTOR QUANTUM DOT CONJUGATES IN BIOSENSING

[1] HEDI MATTOUSSI, PH.D., [1]M. KENNETH KUNO, PH.D., [2]ELLEN R. GOLDMAN, PH.D., [2]GEORGE P. ANDERSON, PH.D. AND [2]J. MATTHEW MAURO, PH.D.

[1]Division of Optical Sciences
[2]Center for Bio/Molecular Science and Engineering
U.S. Naval Research Laboratory
Washington, DC 20375 USA

This chapter reviews progress in bio-related applications of luminescent colloidal quantum dots (QDs). The material reviewed undoubtedly represents only the prologue of an unfolding story, as quantum dots are a relatively recent discovery and their biological applications are newer still. Nonetheless, a significant body of research literature exists pointing the way toward future advances. We begin with a basic introduction to quantum dots, including their synthesis and some characteristic physical properties, then follow with a review of bio-related work involving semiconductor nanocrystals published to-date. Work involving preparation and use of QD-protein conjugates in cellular imaging, quantitative immunoassays, and in early-stage energy transfer applications is reviewed, as well as uses of QD-DNA conjugates as nanoscale building blocks. A listing of early patents in this area is also included for those who contemplate utilizing these materials in the commercial arena. Advantages and limitations in bio-related applications are presented based on the current state-of-the-art in QD technology.

1. Principles of Operation

1.1. Introduction

Once purely a novelty in the realm of low dimensional semiconductor physics, quantum dots (QDs) have now come of age. The last decade has seen tremendous scientific interest and progress in understanding these semiconductor nanoparticle materials as well as initial attempts to develop and commercialize various applications (Yoffe, 1993, 2001; Alivisatos, 1996; Efros et al., 2000; Murray et al., 2000). Prompting this trend has been a growing realization of the technological importance of understanding the chemistry, physics and biology of materials at the nanometer scale, an area collectively known as nanoscience. The drive for expanding our understanding of semiconductor nanocrystals has also been spearheaded by potential applications for these materials in devices such as absorption filters (Borrelli et al., 1987, Hall et al., 1988), light emitting diodes (Colvin et al., 1994; Dabboussi et al., 1995; Schlamp et al., 1997; Mattoussi et al., 1998a), and photovoltaic cells (Greenham et al., 1996).

QD bioconjugates, materials comprised of luminescent colloidal QDs conjugated with biomolecules, can be used in applications such as detection and quantitation of soluble substances, in bioimaging, and potentially, in a range of diagnostics applications. Successful integration of these promising materials into these and other emerging biotechnological areas will necessitate a thorough understanding of the properties of these hybrid bioinorganic systems, requiring multidisciplinary and coordinated efforts in chemistry, physics and materials sciences.

Biological tagging using fluorophores is useful in many biotechnological applications, including immunoassays, disease diagnosis, drug development, and cell and tissue imaging in both single and multiplex approaches (Schrock et al., 1996;, Hermanson, 1996). For instance, recent flow cytometry work (Roederer et al., 1997) using a multi-laser excitation system and a multi-color labeling scheme, allowed concurrent observation of ten parameters involving cellular antigens, demonstrating the high level of sophistication possible using dye labels. Furthermore, microarray-based gene analysis using multiple fluorescent probes has become a critical technology in the burgeoning genomics field (Lobenhofer et al., 2001). Virtually all available organic light-emitting dyes, however, have inherent functional limitations such as narrow excitation bands and broad red-tailing photoluminescence spectra, low resistance to photodegradation, and the necessity for individually tailoring synthesis and conjugation procedures for each fluorophore. Thus, there remains a need for new and improved types of fluorescent labeling materials. Semiconductor nanocrystals (e.g., CdSe-ZnS core-shell QDs) represent a promising alternative in certain bioanalytical and imaging applications (Bruchez et al., 1998; Gerion et al., 2001). These very bright photoluminescent materials have readily tunable spectral properties, high

photobleaching thresholds, and biocompatibility. Colloidal QDs made of ZnSe, CdS, CdSe, CdTe, and HgSe emit light over a wide range of wavelengths in the visible and near IR (Hines et al. 1998; Henglein et al., 1982; Weller et al., 1986; Rosetti et al., 1983, 1984; Murray et al., 1993; Rogach et al., 1997; Mikulec, 1999; Eychmüller et al., 2000). In addition, their essentially continuous absorption envelope allows simultaneous excitation of several different colors of QDs with a single wavelength, making them naturally suitable for multiplexing applications.

In this chapter, we first describe some basic features and unique properties of colloidal semiconductor QDs, followed by a short history outlining some of the most important early bio-related studies. We then present the current status of known research efforts that involve using luminescent colloidal QD bioconjugates in biosensing and bioimaging.

1.2. Chemistry and physics of semiconductor quantum dots

1.2.1. Description. Colloidal semiconductor quantum dots are small, spherical, crystalline particles of a given material consisting of hundreds to thousands of atoms. They are neither atomic nor bulk semiconductors, but may best be described as artificial atoms. Their properties originate from their physical size, which ranges from 10 to ~100 Å in radius and is often comparable to or smaller than the bulk Bohr exciton radius (Woggon, 1997; Gaponenko 1998; Yoffe 2001; Efros et al., 2000). As a consequence, QDs no longer exhibit their bulk parent optical or electronic properties. Instead, they exhibit novel electronic properties due to what are commonly referred to as quantum confinement effects. These effects originate from the spatial confinement of intrinsic carriers (electrons and holes) to the physical dimensions of the material rather than to bulk length scales. One of the better-known confinement effects is the increase in semiconductor band gap energy with decreasing particle size; this manifests itself as a size-dependent blue shift of the band edge absorption and luminescence emission with decreasing particle size (Figure 1).

This size-dependent absorption can be understood by using a simple analogy to a quantum mechanical particle in a one-dimensional box of length L. In this model, a carrier is localized within a potential minimum between two infinite barriers. Due to this spatial confinement, the energies of the carriers are quantized to discrete values, proportional to the inverse of the square of the length of the box ($E_n \propto n^2/L^2$, with n = 1,2,3,…). An extension to QDs is achieved by considering a three dimensional box (or sphere) where the potential minimum represents the QD and the barrier to escape originates from the abrupt termination of the QD at its surface.

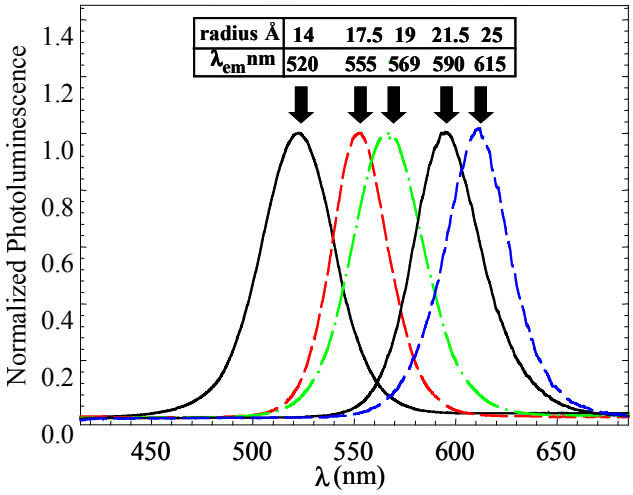

Figure 1. Photoluminescence spectra for five different core sizes of CdSe-ZnS quantum dots in water solutions. All samples were excited at 350 nm. Core radii were extracted from small angle x-ray scattering (SAXS) data (Mattoussi et al., 1998b).

For a spherical QD with an infinite potential barrier one obtains the following expression for the electron and hole energy levels in the particle:

$$E_{l,n}^{e,h} = \frac{\hbar^2 \phi_{l,n}^2}{2m_{e,h}a^2}. \qquad (1)$$

Here $\phi_{l,n}$ is the nth root of the spherical Bessel function of order l, $m_{e,h}$ is the effective mass of the electron (e) or hole (h) and a is the radius of the QD. One therefore predicts discrete quantized electron-hole transitions, an increase in effective band gap (or HOMO-LUMO transition in molecular terms) with decreasing particle size and conversely a decrease in spacing between states with increasing size. It should be noted that the Coulomb interaction between the confined electron and hole alters these energies, but since this term scales as $1/a$, it is essentially a small perturbation to Equation 1, which varies more strongly with size (i.e., $1/a^2$). A number of excellent review articles exist on the subject, particularly those by Yoffe (1993, 2001) Gaponenko (1998) and Efros (Efros et al., 2001); the interested reader is referred to them for more information.

1.2.2. Nanocrystal synthesis. QDs were first discovered in doped silicate glasses by Ekimov and Onuschenko (Ekimov et al., 1980, 1981, 1982, 1983, 1984, 1985a,b, 1993, 1996). In their seminal work, a supersaturated solution of copper and chlorine compounds in glass was heated at high temperatures to cause the controlled precipitation of CuCl. Additional heating of the melt allowed them to

systematically create collections of small crystalline CuCl particles ranging in size from tens to hundreds of angstroms, initially denoted as quantum droplets. The particles have since become known as quantum dots, although alternative names exist in the literature, including nanoparticles, nanocrystals, nanocrystallites and Q-dots. Today, a wide variety of methods such as e-beam lithography, x-ray lithography, molecular beam epitaxy (MBE), ion implantation, sonochemistry, and growth in size-restricted environments are available for making small nanocrystallites not only of semiconductors but also of metals. Some of the more common techniques are outlined below (and in Table 1) with particular emphasis on preparations yielding colloidal QDs that have surface capping/passivating molecules (ligands). Using these ligands allows tailoring of QD solubility in a variety of solvents, permits facile solution processing and can, in some cases, make them amenable to biological manipulations.

Growth of QDs in *glass melts* is achieved by doping the melt with salts of the desired material (Ekimov et al., 1980, 1982, 1986; Borrelli et al., 1987). The temperature of the glass is then rapidly dropped to generate small nuclei of the semiconductor. The glass then undergoes a secondary heat treatment over temperatures ranging from 400 to 1000°C, to induce the nuclei to grow, forming small spherical crystalline particles of semiconductor dispersed in amorphous glass matrices. Advantages of this technique include highly crystalline particles and the ability of the glass host to support very large (hundreds of angstroms) QDs. A serious disadvantage is that the QDs cannot be easily manipulated after their synthesis. They remain trapped in the glass and there are few possibilities for treating the material once made, for example, to alter surface chemistry or improve their size distribution.

In parallel with the discovery of QD growth in glasses, it was found that semiconductor nanoparticles could be grown within *inverse micelles* (Figure 2) (Henglein, 1982; Rosetti et al. 1983,1984; Kotov et al., 1993,1994; Pileni et al., 1992). This technique exploits natural geometrical structures created by water-in-oil mixtures upon adding an amphiphilic surfactant such as sodium dioctyl sulfosuccinate (AOT). By varying the water content of the mixture, it was shown that the size of the water droplets suspended in the oil phase could be varied systematically. This led to the idea of using these self-enclosed water pools as micro-reactors for carrying out nanoscale sustained chemical reactions. In the case of QDs, it was found that adding metal salts to the water pools could cause nucleation and growth of colloidal nanocrystalline particles. Advantages of this technique include reactions carried out at room temperature and, more importantly, the ability to isolate the QDs after their synthesis. The inverse micelle preparation was therefore a significant advance in the development of QDs, giving researchers access to the surface chemistry of the particles for additional functionalization and manipulation.

Table 1. Major known types of Colloidal Group II-VI semiconductor QDs, method of preparation and representative literature citation. Some of these materials have been used in bio-related experiments.

Nanocrystal type	Preparation method	Literature citation
CdS	Silica glass	Ekimov et al., 1985; Potter et al., 1988; Liu et al., 1990, Persans et al., 1989; Zhao et al., 1991
	Aqueous solutions, inverted micelles	Rosetti et al. 1983, 1984, Weller et al., 1986; Misawa et al., 1991; Woggon et al., 1993
	Polymer and high temperature coordinating solutions	Murray et al., 1993; Artmeyev et al., 1995
	Sol-gel glass	Nogami et al., 1990; Minti et al., 1991; Spanhel et al., 1992; Mathieu et al., 1995;Wang et al., 1989; Herron et al., 1989
	Semiconductor-glass composite films	Gurevich et al., 1992
CdSe	Silica glass	Ekimov et al., 1985; Borrelli et al., 1987; Gaponenko et al., 1993
	High temperature coordinating solutions	Murray et al., 1993
	Polycrystalline films	Hodes et al., 1987
CdSe-overcoating	ZnSe using hybrid micelle/organometallic	Kortan et al., 1990
	ZnS using high temperature coordinating solutions	Hines et al., 1996; Dabbousi et al., 1997
	CdS using high temperature coordinating solutions	Peng et al., 1997
CdTe	Silicate glass	Potter et al, 1988; Liu et al., 1991
	Semiconductor-glass Composite films	Ochoa et al., 1996
	High temperature coordinating solutions	Murray et al., 1993; Mikulec et al., 1999
ZnSe	High temperature coordinating solutions	Chestnoy et al., 1986; Hines et al., 1998

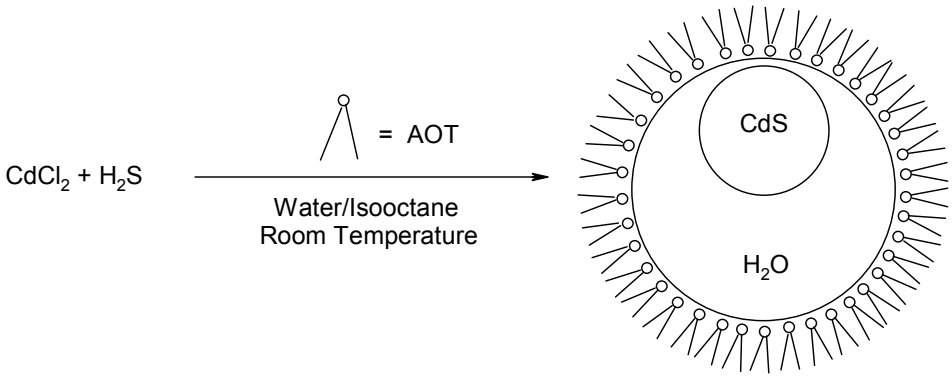

Figure 2. Growth of CdS quantum nanoparticles in inverse micelles. Other materials such as CdSe and CdTe have also been prepared using the inverse micelles approach.

In the early 1990's it was shown by the Bawendi group (Murray et al., 1993) and confirmed shortly thereafter (Bowen Katatri et al., 1994) that an *organometallic synthesis* based on pyrolysis of metal-organic precursors could yield CdSe QDs with a size distribution of 8-10% as made, with distributions that could be improved during post-reaction processing to values as small as 5% (Murray et al., 1995). This preparation followed on the early micelle advances, yielding highly crystalline particles which were significantly improved in terms of their fluorescence quantum yield (QY). Colloidal QDs could now be made with room temperature quantum yields on the order of 5-10% (and low temperature QYs near unity), making fluorescence-based applications of QDs viable for the first time.

This technique is widely used to generate QDs used in bio-related applications, and is described here (Figure 3). In general, a solution of dimethylcadmium ($CdMe_2$) and trioctylphosphine selenide (TOPSe), diluted in trioctylphosphine (TOP), is rapidly injected into a hot stirring solution of trioctylphosphine oxide (TOPO). The rapid introduction and concomitant temperature drop resulting from adding these reagents result in discrete temporal nucleation of CdSe seeds. After reagent injection, the temperature of the solution is raised to 280-300°C in order to grow the particles. The high temperature growth promotes highly crystalline QD cores. Growth is monitored through UV/visible spectroscopy and when the desired size is reached (as monitored by the peak wavelength of the first absorption feature), the temperature is dropped below 100°C to arrest the growth.

A more detailed description of a typical laboratory scale organometallic preparation of QDs is provided in the three steps described below:

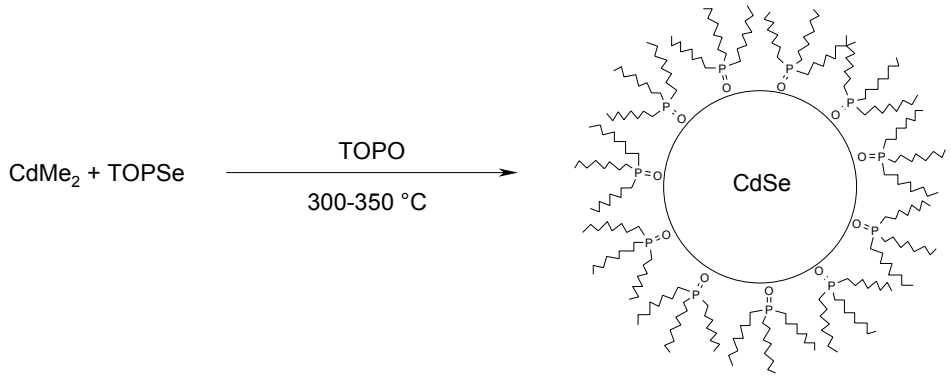

Figure 3. High temperature organometallic growth of colloidal CdSe quantum nanocrystals, as described first by Murray et al. (1993).

1. In a glovebox, under nitrogen, a 1M stock solution of trioctylphosphine selenide (TOPSe) is prepared by adding 7.9 grams of amorphous Se (99.99%) shot to 100 ml of trioctylphosphine (TOP, 90-95%). An injection solution is formulated by adding 170-200 µl $CdMe_2$ and 3.5-4 ml 1M TOPSe to ~15 ml of TOP. The reagents are mixed and loaded into a syringe equipped with a large gauge needle for rapid injection.

2. On a Schlenk line, a 100 ml three-neck flask is loaded with ~20-30 grams of TOPO (90%) and heated to 150-180°C for 2-3 hours under vacuum while stirring in order to remove water. When dry, the flask is backfilled with inert gas (typically N_2) and the temperature is raised to 300-350°C in preparation for precursor injection. The loaded syringe is removed from the glovebox and its contents quickly injected into the flask. Upon injection, there is a vigorous evolution of gas followed by a rapid color change of the solution to light yellow. The temperature falls to ~ 250°C and an absorption spectrum shows sharp features with the peak of the first transition usually located between 470 and 490 nm.

3. The temperature is raised to 290-300°C to allow for growth and annealing of the QDs. During growth, samples are periodically removed and their UV/visible absorption spectra taken. The peak position of the first absorption feature is noted, as well as the relative width of the transition, which gives a measure of a sample's size distribution. Occasionally there is a decrease in the growth rate accompanied by an increase in the relative size distribution. To overcome this growth bottleneck, the temperature is raised by several degrees. When the peak of the first absorption feature reaches a wavelength maximum indicative of a desired size, the temperature is dropped below 100°C to arrest crystal growth.

Recently, Peng and coworkers have developed a modified organometallic synthesis that is less dependent on the purity of the TOPO and avoids the use of pyrophoric $CdMe_2$ precursor (Peng et al., 2001a, Qu et al., 2001). In their synthesis, high purity TOPO and controlled amounts of cadmium coordinating ligands, e.g., hexylphosphonic acid (HPA) or tetradecylphosphonic acid (TDPA), are combined in the preparation flask. Cadmium compounds such as cadmium oxide (CdO) or cadmium acetate [$Cd(Ac)_2$] are added at a relatively low temperature (e.g., at 140°C) and the mixture heated to generate Cd^{2+} ions before addition of TOPSe results in nanocrystal nucleation and growth. This procedure is promising; however, additional work is still needed before reproducible high quality CdSe and CdSe-ZnS QDs can be routinely prepared.

To obtain material with low size dispersity, growth of CdSe QDs is often followed by size selective precipitation (Murray et al., 1993). This involves adding a "bad" solvent for the TOP/TOPO-capped nanocrystals, such as methanol, to a preparation of QDs whereupon larger particles in the mixture precipitate first due to preferential Van der Waals interactions. Smaller particles remain in solution until enough MeOH is added to drive most of the QDs out of solution. Use of size-dependent QD precipitation enriches for populations of desired nanocrystal size. Repeated precipitations can reduce the overall size distribution of QD synthetic mixtures to values of ~5%. This method is widely employed for polymers and colloids to reduce polydispersity after synthesis. Size and size distribution measurements are usually carried out using transmission electron microscopy (TEM) (Murray et al., 1993) and/or small angle x-ray scattering (SAXS). TEM tends to provide slightly smaller values for the inorganic core than SAXS because TEM does not take into account the amorphous outermost atomic layer on the nanocrystal surface (Mattoussi et al., 1998b).

It was discovered in the mid-1990's that passivating QDs with an additional thin layer made of a wider band gap semiconductor could improve the surface quality of the particles (by providing a better passivation of surface states), resulting in dramatic enhancements of the fluorescence quantum yield. Although the principle was previously known from semiconductor bandgap engineering (Steigerwald et al., 1988; Kortan et al., 1990), the optimal set of conditions for creating strongly fluorescent overcoated QDs was not realized until the seminal work of Hines and Sionnest (Hines et al., 1996), when they showed that overcoating CdSe QDs with ZnS improved quantum yields to values of 30% or greater. This was shortly followed by other studies that described additional characterization of CdSe QDs overcoated with ZnS (Dabbousi et al., 1997) and CdS (Peng et al., 1997).

In brief, the procedure for overcoating colloidal QDs with another semiconductor involves the following steps. A dilute solution of QDs is made up in an appropriate coordinating solvent (TOPO, for instance). The temperature of the

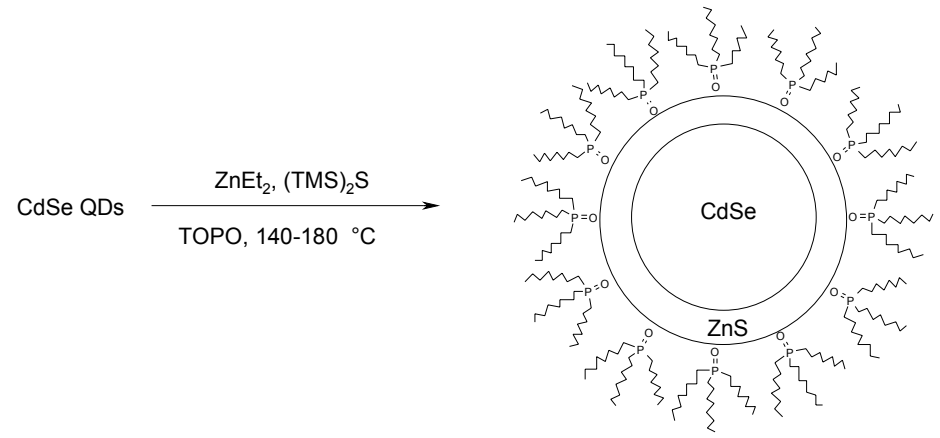

Figure 4. Overcoating of CdSe quantum dots with ZnS using high temperature solution route.

solution is raised to ~150°C but kept lower than 200°C to prevent further growth of the QDs. A dilute solution of Zn (or Cd) and S precursors is then slowly introduced into the hot stirring QD solution. The high dilution and relatively low temperature of the mixture prevent separate nucleation of ZnS or CdS quantum dots. Once the precursors have been added, the temperature is lowered to ~ 80°C and the reaction vessel left undisturbed for several hours. Noticeable improvements in the PL quantum yield are apparent after several hours of heat annealing (Figure 4).

A typical laboratory scale ZnS overcoating process for CdSe QDs includes the following steps (Dabbousi et al., 1997): Size-selected CdSe particles dispersed in hexane are added to 5-10 grams of dried, degassed TOPO at ~70°C. Inside the glovebox, equimolar amounts of diethylzinc (or $CdMe_2$) and hexamethydisilathiane are mixed with ~5 mls of TOP. The amount of Zn and S precursors added varies depending on the size of the CdSe QD and is calculated to yield a 2-3 (or more) atomic monolayer coverage on the particle surface. Once this solution has been prepared, the temperature of the QD/TOPO solution is raised to a value between 140°C and 180°C. The Zn (Cd) and S precursor solution is then brought out of the glovebox and introduced at a rate of ~ 0.5 ml/min through a separate addition funnel attached to the flask holding the QD/TOPO mixture. Once the addition is complete, the pot temperature is lowered to ~80°C, and the mixture is left undisturbed for several hours. The overcoated QDs are subsequently precipitated with methanol prior to further processing.

1.3. Semiconductor nanocrystal properties

Initial optical studies of QDs in the late 1980's aimed at correlating size-dependent spectral shifts in absorption with quantum confinement effects. Today, the absorption properties of CdSe QDs are relatively well understood with up to ten excited states in the absorption assigned and theoretical avoided crossings observed (Norris et al., 1996). However, the origin of the band edge emission in CdSe QDs was not immediately understood due to the inability of the same theory to explain unusual size-dependent features in QD fluorescence spectra. This presented a serious challenge to the above model, and it was not until the mid 1990's, when Chamarro (Chamarro et al., 1995, 1996) realized the importance of electron hole exchange interaction in QD materials that a more comprehensive understanding of CdSe QDs was achieved. Modifications by Efros to that theory led to understanding of previously unrecognized "dark exciton" effects, which explained many unusual features in the emission spectra such as the size-dependent "resonant" and "global" Stokes shift observed in fluorescence line narrowing and global excitation experiments (Nirmal et al., 1995; Efros et al., 1996; Kuno et al., 1997).

In 1996 Nirmal et al. conducted the first single-particle fluorescence studies of isolated TOP/TOPO-capped CdSe and CdSe-ZnS QDs. They discovered that QDs underwent intermittent on/off emission (so-called "blinking") under continuous excitation (Nirmal et al., 1996). Unlike single fluorescent molecules, this behavior could not be attributed to a commonly known effect referred to as quantum jumps (Cook and Kimble, 1985). Instead, the on/off intermittency in QD emission was attributed to Auger ionization of the QD (Chepic et al., 1990; Nirmal et al., 1996; Efros et al., 1997). The blinking effect is still not fully understood, however.

2. History of Bio-Related Applications using QD Bioconjugates

The amount of published research involving bio-related uses of semiconductor nanocrystals has expanded rapidly since the initial reports from the laboratories of Alivasatos (Bruchez et al., 1998) and Nie (Chan and Nie, 1998) first appeared. This section begins with a description of early work on the preparation of protein-derivatized water-compatible quantum dots, preliminary QD-protein conjugate characterization and their use in imaging cellular structures. It is followed by description of a simple and useful electrostatically controlled conjugation method developed in our laboratory (Mattoussi et al., 2000). We conclude by describing briefly the original work involving formation and use of QD-DNA conjugates as performed in the Mirkin laboratory (Mitchell et al., 1999).

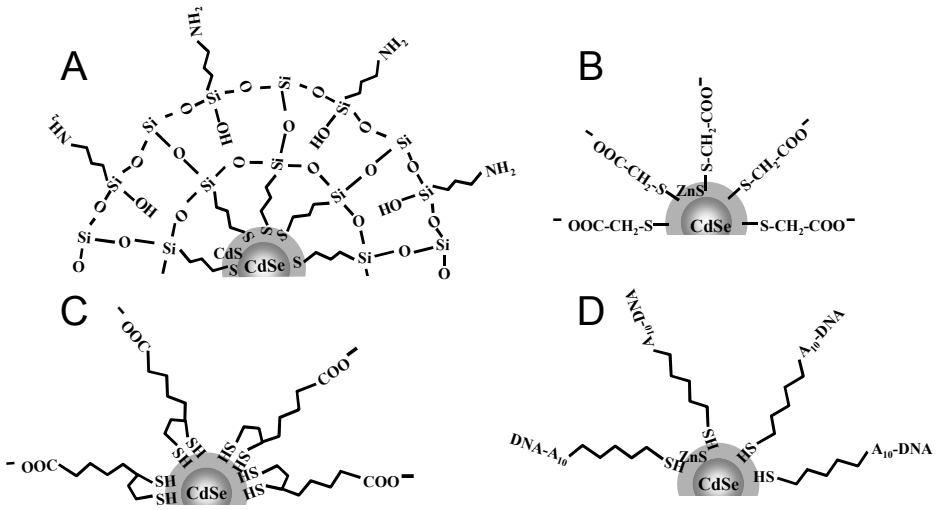

Figure 5. Surface treatment of overcoated quantum dots. A) Silica shell with reactive amine functions; B) Mercaptoacetic acid coverage; C) Capping with dihydrolipoic acid [DHLA]. D) Direct binding of thiol-terminated DNA.

2.1. Preparation and use of QD bioconjugates in cellular imaging

Water-soluble nanocrystals derivatized with the actin-binding protein, phalloidin, were used for the first attempts at intracellular imaging in fixed mouse fibroblasts (Bruchez et al., 1998). For conjugating phalloidin with nanocrystal surfaces, the authors started with CdSe-CdS core-shell QDs that were capped with a thin amine-derivatized silica shell to render them both reactive and water-compatible (Figure 5A). The silica-encapsulated, red-emitting CdSe-CdS core-shell particles (4 nm diameter core size and emission maximum at 630 nm) were subsequently biotinylated at their exposed reactive amine sites. Streptavidin was then used effectively as a bridge between actin-bound biotinylated phalloidin and the biotinylated red-emitting QDs in cell imaging work. Simultaneous nuclear staining was achieved using green-emitting QDs coated with an anionic silane, in a process driven by electrostatic and hydrogen binding interactions. Light from a mercury lamp with a 488 nm excitation filter and a single long-pass emission filter were used to image both red (actin-bound) and green (nucleus-bound) QDs at the same time. Importantly, it was also demonstrated with sequential scans using laser scanning confocal microscopy that the red nanocrystal bioconjugates were dramatically more photostable than fluorescein-labeled phalloidin bound to actin fibers under essentially identical conditions. A detailed description of the process used for preparation of silica encapsulated reactive QDs, together with more extensive characterization of their properties, has since been published (Gerion et al., 2001).

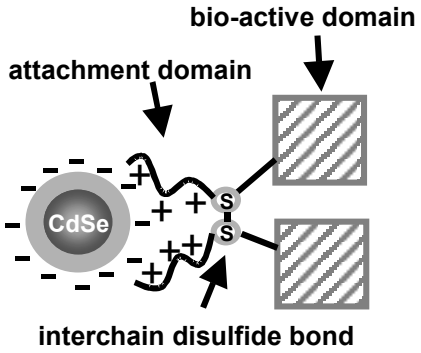

Figure 6. Schematic of engineered two-domain protein electrostatically complexed with a DHLA-capped CdSe-ZnS quantum dot (based on Mattoussi et al., 2000).

A contemporaneous imaging study employed bio-compatible nanocrystals conjugated with human transferrin to conduct intracellular staining of fixed HeLa cells (Chan and Nie, 1998). For conjugating transferrin with nanocrystal surfaces, the authors started with CdSe-ZnS core-shell dots that had been capped by ligand-exchange with mercaptoacetic acid in order to render them both water-compatible and reactive (Figure 5B). Mercaptoacid-capped red-emitting CdSe-ZnS core-shell particles (2.1 nm radius and emission maximum of 560 nm) were subsequently coupled with transferrin using 1-ethyl-3-(3-dimethylaminopropyl carbodiimide) hydrochloride (EDC)-promoted condensation chemistry. The conjugates preserved the absorption and photoluminescence properties of the nanocrystals as well as the activity of the transferrin. For QD-transferrin conjugates, functionality was demonstrated by exposing the conjugates to cultured HeLa cells overnight followed by extensive washing and imaging using an epifluorescence microscope equipped with a CCD camera. Imaging revealed that luminescent QDs had entered the cells, presumably via receptor-mediated endocytosis. In the absence of transferrin, i.e., using capped 2.1 nm core radius QDs without a protein coating, only weak cellular autofluorescence was observed. These authors also prepared human IgG-QD conjugates using the same methods. Reaction with human IgG-specific polyclonal antibody resulted in extensive aggregation as observed using fluorescence imaging, undoubtedly due to inter-dot bridging among multiply-derivatized QDs.

2.2. Preparation of QD-protein conjugates using a non-covalent strategy

An alternative method for preparing functional QD-protein conjugates has been developed in our laboratory at NRL. This system employs “bidentate” dihydrolipoic acid (DHLA) groups to coat QDs (Figure 5C) in combination with two-domain proteins engineered to interact electrostatically with negatively

charged QD surfaces. In a model system that employed engineered variants of *E. coli* maltose binding protein (MBP) and DHLA-capped CdSe-ZnS nanocrystals, stable self-assembled QD-protein complexes formed in an efficient and controlled manner (Mattoussi et al., 2000). In order to promote the self-assembly process, a modular MBP-basic leucine zipper chimeric protein was designed and prepared in a recombinant system (MBP-zb) (Figure 6). The strongly positively-charged C-terminal "tail" present in the novel MBP-zb variant resulted in rapid formation of QD-MBP conjugates that retained both the optical QD properties and the active folded state of the MBP protein. Based on incremental increases in fluorescence quantum yield that occurred upon titration of QDs with increasing amounts of MBP-zb, and from steric considerations, it was estimated that for a nanoparticle of ~ 70 Å (core-plus-shell) diameter an average of 12-15 engineered protein molecules could be packed around each nanocrystal (Mattoussi et al., 2001). That number can presumably increase or decrease for larger or smaller QDs, respectively.

In the first known use of QD-bioconjugates in a quantitative fluoroassay, a functional assay for maltose was developed that monitored displacement of QD-MPB-zb conjugates bound to a cross-linked amylose affinity matrix as various amounts of dissolved maltose were injected into the flowing buffer upstream of the affinity column. Maltose concentrations of injected samples were determined by integrating PL intensity (QD emission) versus time as QD-MBP-zb conjugates were displaced from the column by maltose; limits of detection were on the order of 10 pmol of maltose (Mattoussi et al., 2001).

In order to prepare reagents for use in fluoroimmunoassays, an analogous recombinant construct was developed based on the IgG-binding domain of protein G from *Staphylococcus*. In this construct, the engineered dimeric form was critical in providing two points of attachment for each IgG. The PG-zb protein serves as a very effective bridge between the DHLA quantum dot surface and any type of IgG antibody, resulting in reagents that can be used in general fluorimmunoassay protocols. QD-antibody complexes made with this strategy were used in fluoroimmunoassays in analysis of the protein toxin staphylococcal enterotoxin B (SEB) (Tran et al., 2001; Goldman et al., 2001, 2002a) and in analysis of low levels of 2,4,6-trinitrotoluene (TNT) and hexahydro-1,3,5-trinitro-1,3,5-triazine (RDX) dissolved in water (Goldman et al., 2002a,b). In the sandwich-assay format for SEB, the limit of detection was about 200 pmol of the protein toxin. A competition assay performed in microtiter plates for TNT and RDX allowed facile quantitation of the dissolved explosives, with detection limits of 1 ng and 0.2 ng of the explosives, respectively (Goldman et al., 2002a).

2.3. QD-DNA conjugates

Sequence-dependent hybridization of deoxyoligonucleotides bound to CdSe-ZnS QDs was first demonstrated in the Mirkin laboratory (Mitchell et al., 1999). Two

populations of nanoparticles were prepared using either 3' or 5' alkyl thiol-terminated 22-mer oligonucleotides for QD surface attachment (Figure 5D). Upon addition of a 24-mer "bridging" or "capture" oligonucleotide designed to be complementary to the outer 12-mer sequence of both types of DNA-modified nanoparticle, a cross-linked network of specifically hybridized particles was formed. Aggregation was demonstrated to be specific by control experiments with non-complementary capture DNA in which no evidence of multi-center cluster formation was observed. Cluster formation by specific hybridization resulted in a decrease in integrated fluorescence intensity of 26 ± 6%; excimer formation between the DNA linked dots was cited as a possible explanation.

These researchers also broke new ground by forming and characterizing mixed aggregates composed of both QD-DNA and Au-DNA conjugates. Temperature-induced melting of the hybridized DNA present within both QD-oligonucleotide complexes and mixed QD-Au nanoparticle-DNA complexes was studied by monitoring light absorption versus temperature. A sharp duplex melting temperature transition was observed, suggesting that cooperativity effects operate within the complexes due to multiple DNA links per particle. Melting of mixed QD-Au-DNA particles ("A-B" structures) could be observed at one tenth the concentration of a pure QD-DNA system due to the very large molar extinction coefficient associated with the plasmon band of the DNA-derivitized 13 nm Au particles used (2.8×10^8 M^{-1} cm^{-1}). Construction of more complex multicomponent nanostructured materials might be possible using these types of building blocks.

2.4. Seminal patents

Although applications of quantum dots to bio-related issues is a relatively new area, several U.S. patents have already been issued for processes involving synthesis and use of quantum dots within the biochemical realm. Table 2 presents eight seminal patents in the area. All have been issued within the last two years. A wide range of areas is covered in these patents; interested readers should consult the U.S. Patent and Trademark Office Home Page (http://www.uspto.gov/) for viewing the complete patents.

3. State of the Art

3.1. Types of QDs and their optical properties

Colloidal semiconductor nanocrystal quantum dots are in general considered to be spherical in shape. They can be dispersed in a solid matrix such as those prepared by annealing at high temperature in glasses (referred to as quantum droplets), where the nanocrystal growth is driven by precipitation/nucleation, or

Table 2. Seminal patents describing applications involving the use of QD-conjugates.

Patent Number	Issue Date	Patent Title	Authors/Assignees
6,309,701	Oct. 2001	Fluorescent nanocrystal-labeled microspheres for Fluorescence analysis	E. Barbera-Guillem/ Bio-Pixels, Ltd.
6,207,392	Mar. 2001	Semiconductor nanocrystal probes for biological applications and process for making and using such probes	S. Weiss, M. Bruchez, P. Alivisatos/ Univ. of California
6,319,607	Nov. 2001	Purification of functionalized fluorescent nanocrystals	E. Barbera-Guillem/ Bio-Pixels, Ltd.
6,306,610	Oct. 2001	Biological applications of quantum dots	M. Bawendi, F. Mikulec, V. Sundar/ MIT
6,274,323	Aug. 2001	Method of detecting an analyte in a sample using semiconductor nanocrystals as a detectable label	M. Bruchez, R. Daniels, S. Empedocles, V. Phillips, E. Wong,, D. Zehnder/ Quantum Dot Corp.
6,319,426	Nov. 2001	Water-soluble semiconductor nanocrystals	M. Bawendi, F. Mikulek, J. Lee/ MIT
5,990,479	Nov. 1999	Organo Luminescent semiconductor nanocrystal probes for biological applications and process for making and using such probes	S. Weiss, M. Bruchez, P. Alivisatos/ Univ. of California
6,114,038	Sept. 2000	Functionalized nanocrystals and their use in detection systems	S. Castro and E. Barbera-Guillem/ BioCrystal Ltd.

surface functionalized with organic ligands to make them soluble in a variety of organic solvents to make colloidal dispersions. The latter are usually grown using inverted micelles or high temperature solution chemistry routes. Recently, preparation of anisotropic semiconductor nanocrystals made of CdSe (quantum rods) using the organometallic synthesis route was reported. Control of the type of cadmium ligands used (e.g., HPA or TDPA) and the concentration of the cadmium complexes formed are the key elements to growing anisotropic

nanocrystals (Peng et al., 2000, 2001b). These quantum rods were reported to have linearly polarized luminescence emission, a property that may have a potential use in biological tagging applications (Hu et al. 2001).

The common optical property that characterizes QDs is the size-dependence of their spectroscopic properties (e.g., absorption and phohtoluminescence), which results from quantum confinement of charge carriers within a volume smaller or comparable to the Bohr exciton radius. Within the family of II-VI compounds the range of absorption and emission peaks depends on the materials; ZnS and ZnSe QDs have absorption and emission spectra limited to the UV and blue regions, whereas nanocrystals made of heavier atoms such CdTe or HgSe or hybrids composed of PbSe (III-VI compounds, Murray et al. 2001b) have useful optical properties that extend into the near IR region of the spectrum. For biological labeling, colloidal CdSe-ZnS QDs have been the most widely used in published studies. Experiments using CdS QDs, CdS-overcoated CdSe nanocrystals or CdTe QDs have also been described in a few instances (Mahtab et al., 1996, Bruchez et al., 1998, Mamedova et al., 2001).

3.2. Nanocrystal surface treatment

3.2.1. Inorganic overcoating. For colloidal nanocrystals, organic ligands tend to provide only partial surface passivation, which translates into rather modest photoluminescence yields. Overcoating the native core with a wider band gap semiconducting material provides additional surface passivation and reduces leakage of excitons outside the core. Optimal passivation of the surface states occurs when the growth of the overcoating layer is near-epitaxial, i.e., the lattice mismatch between the core and the shell material is as small as possible. On the other hand, using an overcoating material that has a closely matching lattice structure in order to promote epitaxial growth produces a leakage of the exciton to the overcoating layer, which in turn results in a pronounced red shift of absorption and emission spectra in comparison with the native nanocrystals. This pronounced red shift has an additional disadvantage as it moves the range of useful wavelengths further into the red. For example, when using a CdSe core, overcoating with CdS produces a higher PL yield than the one measured with ZnS. However, minimal red shift of the band edge absorption and emission are measured for CdSe-ZnS QDs compared with CdS-overcoated nanocrystals. Thus, only ZnS-overcoated QDs allow a broad range of wavelengths in the visible to be produced including emission in the blue region of the optical spectrum.

3.2.2. Capping ligands for bio-compatibility and conjugate formation. Protecting the nanocrystals' physical and chemical integrity in aqueous media, while simultaneously providing sufficiently reactive surface sites to allow bioconjugation, has been challenging. Several means of accomplishing this have been devised, some of which have already been alluded to. Capping with

mercaptoacids imparts water solubility and provides carboxyl groups for the condensation chemistry necessary for further covalent modification (Chan and Nie, 1998) (Figure 5B). It has been suggested that the "bidentate" type of interaction of dihydrolipoic acid (DHLA) (Figure 5C) (Mattoussi et al., 2000) or dithiothreitol (Pathak et al., 2001) with the inorganic QD surface results in more water-stable nanocrystals, but no systematic study has been performed. The charged surface provided by DHLA-capped CdSe-ZnS QDs drives electrostatic self-assembly of QD-protein conjugates that, once formed, are surprisingly stable even in high salt solutions (Mattoussi et al., 2000).

Porous silica shells have been used for passivation and placement of hydroxyl, amino, thiol, and phosphonate groups in position for bioconjugate formation (Gerion et al., 2001) (Figure 5A). Attachment of thiolated DNA directly to QDs by replacement of surface mercaptoacids has been successfully accomplished (Figure 5D) (Mitchell et al., 1999), and similarly, CdS nanoparticles have been grown in the presence of thiolated peptides, resulting in derivatized fluorescent particles able to recognize cellular receptors (Winter et al., 2001).

3.3. Bioassay work involving quantum dots

Quantum dot bioconjugates can function as fluorescent reporters in recognition-based quantitative and qualitative bioassays. QDs conjugated to both proteins and DNA have been used in a limited number of applications, as described below.

3.3.1. Fluoroimmunoassays using QD-antibody conjugates. Immunoassays utilizing CdSe-ZnS QD-conjugates formed by electrostatically driven self-assembly have been developed (Goldman et al., 2001, 2002a, b; Tran et al., 2001). QD-antibody complexes for use in bioassays have been formed using adaptor proteins as bridges to link QDs with antibodies. Either naturally occurring protein bridges (e.g., avidin) or engineered recombinant protein bridges can be used in this capacity. In practice, mixed-surface QD conjugates have been made with both the antibody-binding adaptor protein and an engineered maltose binding protein derivative (MBP-zb) bound to their surface (Figure 7A). The mixed recognition elements on the particles allow separation of QD-antibody complexes from unbound antibody using affinity chromatography. After saturation of antibody binding sites with IgG (or biotinylated IgG when using the avidin bridge) and purification on a cross-linked amylose column to remove excess unbound IgG, various QD-antibody conjugates have been demonstrated to bind antigen directly adsorbed to microtiter plates. Sandwich- or competitive-type assays were then performed in model systems for analysis of staphylococcal enterotoxin B (SEB) and for detecting low levels of the explosives TNT and RDX dissolved in water (Figure 7B and Figure 8).

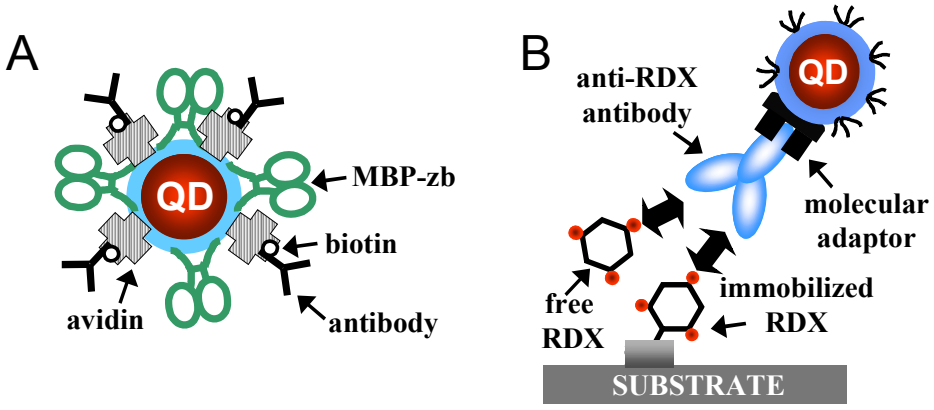

Figure 7. QD antibody conjugates prepared using molecular bridges. A. Mixed surface conjugate after purification by cross-linked amylose affinity chromatography. B. Schematic of competitive assay for the explosive RDX dissolved in water (Goldman et al., 2002a,b).

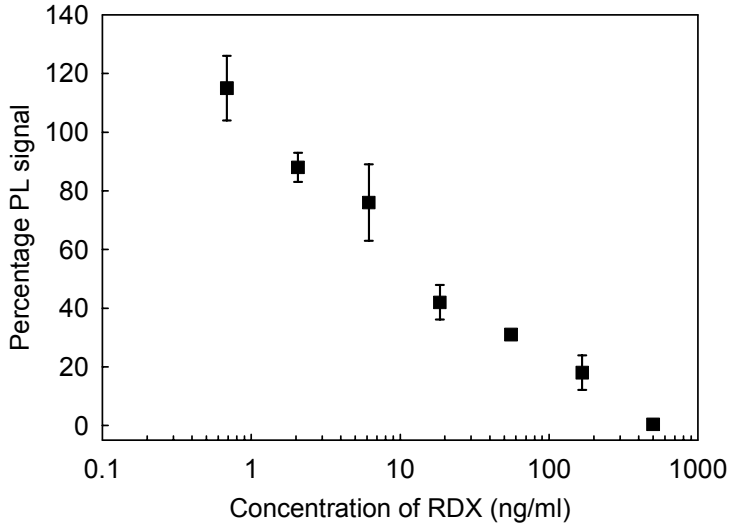

Figure 8. Results of a quantitative competitive assay for RDX using QD-anti-RDX antibody conjugates, where inhibition of QD-conjugates to BSA-RDX by free RDX was investigated. 100% indicates signal in the absence of RDX.

Laser scanning confocal microscopy has also been used as the means of detection in sandwich immunoassays utilizing QD-antibody conjugates (Sun et al., 2001). In these experiments, rabbit anti-human antibody was covalently conjugated to CdSe-ZnS core-shell QDs using EDC chemistry; unconjugated antibody was removed using repeated cycles of washing and centrifugation. Rabbit anti-human IgG was immobilized on a glass slide to form the capture layer, followed by exposure to a mixture of human IgG and goat IgG. After incubation and rinsing unbound antibodies, the surface was exposed to a solution of QDs conjugated with rabbit-anti-human antibodies. Reading the fluorescence signal of the glass slide showed a linear increase of the signal with human IgG concentration, indicating that the QD-conjugates specifically recognized immobilized human IgG. IgG samples containing about 2 μg/ml antibody could be detected. Comparison against antibody labeled with a conventional fluorophore (fluorescein isothiocyanate) in the same system gave a limit of detection of about 25 ng/ml. Inappropriate selection of the excitation wavelength with respect to the absorption and emission of the nanocrystal employed in the assay may have contributed to reduced assay sensitivity with the QD conjugates.

CdS QDs prepared with amino-derivatized polysaccharides (aminodextrans, Amdex) have been conjugated with mouse monoclonal anti-T4 antibody for use in flow cytometry (Sondi et al., 2000). The QD-Amdex-antibody complexes were purified from unconjugated antibody by size exclusion chromatography. Samples of whole blood were lysed and the anti-T4 antibody-Amdex-QD reagent tested for the detection of T4 positive lymphocytes. For unknown reasons, direct cytometric detection using QD fluorescence was not achieved. Signal was seen, however, when sheep-anti-mouse antibody conjugated to phycoerythrin was added to the sample containing anti-T4 antibody-Amdex-QDs, suggesting that the purified QD conjugates were effectively binding to receptor sites on the lymphocytes.

3.3.2. DNA-based systems using QDs as reporters. QDs have been used as probes of DNA structure (Mahtab et al., 1996; Gearheart et al., 2001). Luminescence from CdS QDs was monitored as DNA with different sequences (implying different local structures) was adsorbed to QD surfaces. Adsorption of increasing amounts of DNA to QD surfaces resulted in systematic decreases in emission intensity. DNA sequences with intrinsically kinked structures were found to bind preferentially to nanoparticles rich in surface Cd^{2+} sites as well as to neutral, mercaptoethanol-capped CdS QDs. DNA molecules lacking kinks, however, bound to the Cd^{2+}-rich surface of CdS QDs and not to mercaptoethanol-capped QDs. DNA methylation affected the interaction of Cd^{2+}-rich surfaces of CdS QDs with DNA. Addition of DNA containing hypermethylated triplet repeats $d(^{m}C^{m}CG)_7$ to QDs produced less quenching of the particle luminescence than equal amounts of $d(^{m}CGG)_7$ DNA, even though the binding constants for the two types of DNA were essentially identical.

In another demonstration of the use of QD-DNA conjugates, DNA conjugated to CdSe-ZnS QDs have been used for the detection of specific chromosome sequences in human sperm cells using fluorescence *in situ* hybridization (FISH) (Pathak et al., 2000). Prior to DNA conjugation, the nanoparticles were treated with dithiothreitol, presumably resulting in stable "bidentate" interactions of each capping molecule with the ZnS overcoating. Surface hydroxyl groups made available by this process were then activated with carbonyl diimidazole (CDI) and reacted with 5'aminated oligonucleotides to give stable carbamate linkages. QD-oligonucleotide conjugates with sequences specific for the Y-chromosome were used in FISH assays on human sperm cells. Half the cells are expected to contain a Y chromosome and hybridize to the probe, while the other half should contain the X chromosome and should not hybridize with the probe. As predicted, about half the cells showed the fluorescent signal. Only background emission (less than 5% of positive signal) was seen when identical experiments were performed using unconjugated QDs or QDs conjugated to an oligonucleotide having a non-relevant sequence, i.e., a sequence not present in the human genome.

3.4. Bio-imaging applications using quantum dots

The two pioneering efforts described in the History section of this review have demonstrated in a "proof-of-principle" mode the utility of using quantum dot bioconjugates as histochemical imaging reagents (Bruchez et al., 1998; Chan and Nie, 1998).

In a logical extension of initial cell imaging work, specific sites on the surface of living cultured neuronal cells have been labeled with CdS quantum dots derivatized with two types of recognition molecules (Winter, et al., 2001). In the first case, primary antibodies directed toward the α_v subunit of the $\alpha_v\beta_1$ integrin that studs the surface of SK-N-SH neuroblastoma cells were treated with secondary antibody-QD complexes. Specific attachment of QDs was verified by bright field and fluorescence optical microscopy. In an effort to reduce the distance between QDs and the cell body, CdS dots were prepared in the presence of synthetic peptide CGGGRGDS, which includes the RGD (Arg-Gly-Asp) sequence known to bind to $\alpha_v\beta_1$ and $\alpha_v\beta_3$ integrins as well as a terminal cysteine residue for interaction with exposed surface atoms of the nanocrystal. Preparation of these peptide-derivatized nanoparticles was performed by single-step arrested precipitation in the presence of 1:10 peptide:mercaptoacetic acid; fluorescence anisotropy studies of the prepared particles strongly suggested that peptide attachment had in fact occurred. Microscopy of the cells following exposure to the RGD dots showed a yellow/orange layer of CdS dots coating the blue autofluorescent cells. The control with a non-binding peptide sequence was negative for the staining. Although the thrust of this work involved demonstration of specific binding to living cells, long-range goals involve

preparation of nerve cell-semiconductor interfaces for use in future nanodevices and sensors.

Time-gated imaging of mouse fibroblast cells has been accomplished using silanized 1.8 nm radius (575 nm peak emission) CdSe-ZnS quantum dots (Dahan et al., 2001). In preliminary experiments, the normalized fluorescence decay for the particles used was fit with a triple exponential with components of 3.4, 16.1, and 35.6 ns, corresponding to 1, 50, and 48 percent, respectively, of the emitted photons. Mouse 3T3 fibroblasts incubated overnight with 10 – 100 nM nanocrystals were washed and fixed prior to image collection using a custom built stage-scanning time-correlated single-photon counting confocal microscope. Images constructed using all detected photons (i.e., no time gating) showed dense non-specific autofluorescence throughout the cells, while images constructed with photons from the 35-65 ns window exhibited very low backgrounds with isolated bright clusters of QDs. These aggregated QDs were possibly taken up by the growing cells via endocytosis and stored in lysozomes. Time gating resulted in a 15-fold enhancement in signal-to-noise over the ungated data. Enhanced image constrast will likely be crucial to observing single-nanocrystals in cellular environments.

3.5. Energy transfer and quenching studies

Solution phase protein-ligand binding models have been studied using CdSe-ZnS QDs conjugated to proteins by monitoring fluorescence resonance energy transfer (FRET) between a QD energy donor conjugated to one binding partner and an organic acceptor dye attached to the other binding partner (Willard et al., 2001). Biotinylated bovine serum albumin (bBSA) was conjugated to the QDs by introduction of free sulfhydryl groups onto the protein; the new thiol groups served as attachment points for the protein to the QD surface. Unconjugated bBSA was removed by filtration through a 100 kD cutoff spin column. Introduction of increasing concentrations of streptavidin labeled with tetramethylrhodamine (TMR) to purified QD-bBSA conjugates resulted in decreases in the QD fluorescence emission. A concurrent increase in the TMR emission was observed, suggesting that energy transfer was occurring.

Energy transfer between a fluorescent protein donor (BSA) emitting in the near UV and CdTe QDs was studied in aqueous solutions of QD-BSA conjugates (Mamedova et al., 2001). BSA emission is centered at 340 nm and originates from naturally occuring tryptophan residues. CdTe nanocrystals, prepared using arrested precipitation, were capped with L-cysteine and conjugated with BSA using a one-step linkage procedure employing glutaric dialdehyde, which forms a bridge between the amino groups on the L-cysteine and the lysine moieties on the BSA. The coupling procedure preferentially yielded a 1:1 stoichiometery BSA-QD conjugates with a small fraction of 2:1 (BSA:QD) complexes. When the BSA-CdTe conjugate solutions were excited at 290 nm, where both protein and

QD absorb, emission from the BSA was completely quenched, while that of the QDs showed a two-fold increase with respect to unconjugated nanocrystals. In controls using unconjugated QDs (i.e., unlinked with protein) BSA emission persisted, but only ~ 1/3 of its value measured in the absence of QDs, while QD emission was unaffected. The decrease in the BSA emission was attributed to changes in the pH and presence of Cd^{2+} ions, which alters the luminescence efficiency of tryptophan residues. Excitation at longer wavelengths, where BSA absorption is negligible, showed only emission from the nanocrystals. The authors attributed the above observation to resonance energy transfer from BSA to CdTe QD in the QD-BSA complexes.

Solution-phase fluorescence quenching assays have been carried out using a dye-labeled variant of the two-domain maltose binding protein (MBP), MBP-tb A75C, bound to DHLA-capped CdSe-ZnS quantum dots. The protein variant, which contained a single cysteine, was specifically labeled at that residue with the non-emitting quencher dye QSY-7 (Tran et al., 2002). Conjugation of MBP-tb and DHLA-capped QDs was driven by electrostatic self-assembly. QSY-7 was chosen as a quenching chromophore due to the overlap between its absorption spectrum and the emission spectrum of the QDs employed (core radius of 21.5Å and emission maximum centered at 590 nm). Increased quenching of the nanocrystal emission was observed with increasing amounts of quencher-labeled protein bound; the nanocrystals lost about 90% of their signal when 60% of the MBP-tb QD-bound molecules were QSY-7 labeled (Figure 9). When all the conjugated proteins (ca. 5 per QD) were labeled with QSY-7, the nanocrystal emission was nearly fully quenched. These results were attributed to radiationless energy transfer occurring between the QDs and bound MBP-tb/QSY -7.

In a second system, the emission from surface-tethered QDs was monitored as QSY-7-labeled antibodies were bound to immobilized nanocrystals using an antibody-specific molecular adaptor PG-zb (Tran et al., 2002). DHLA-capped QDs were first immobilized on poly-L-lysine-treated glass slides, followed by incubation with PG-zb to form QD-PG-zb conjugates. The surface-bound QD-PG-zb complex has a high selectivity for the F_c region of antibodies, and introduction of the QSY-7-labeled antibodies onto these surfaces resulted in formation of labeled QD-PG-zb-IgG conjugates. Fluorescence quenching occurred systematically as the proportion of QSY-7 labeled IgGs conjugated to surface-bound QDs increased, until all available QD surfaces had been saturated with labeled antibody (Tran et al., 2002).

3.6. QDs in polymerized microspheres for use as micro-barcodes

Bio-related applications of microsphere-encapsulated quantum dots have recently been investigated (Han et al., 2001). CdSe-ZnS nanocrystals were embedded in cross-linked polymeric beads (1-2 μm diameter size) formed by emulsion

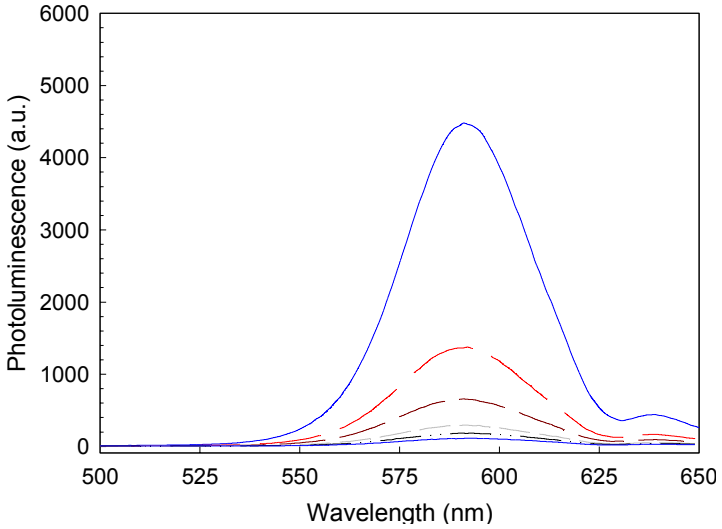

Figure 9. PL spectra of solutions in a 2 mm optical path cell containing 30 pmol QDs and increasing molar ratio of QSY-7-labeled MBP-tb to QD. The total numbers MPB-tb proteins per QD remained fixed (protein to QD ratio of 5). The highest PL intensity was measured in solution containing unlabeled QD-MPB-tb conjugates, and the signal decreased systematically with increasing fraction of labeled proteins, with QSY-7-MBP-tb varying from 0 (unlabeled proteins) to 5 (100% QSY-7-labeled proteins) in the above data.

polymerization of styrene, divinylbenzene and acrylic acid. The process of embedding the nanocrystals involved swelling the beads in a solution of chloroform and butanol in the presence of one or more populations of nanocrystals. Nanoparticles that had migrated into the swelled spheres were trapped upon removal of solvent. The relatively large size of the polymer spheres allowed embedding of a large number of QDs in each bead. Using a single dot size (thus one color), a range of intensity-coded beads could be prepared. Embedding two, three, or more populations of QDs per bead allowed control of the emission intensity and detailed spectral characteristics of the QD-beads, resulting in sets of "color and intensity barcode" polymer beads.

A model DNA hybridization system using oligonucleotide probes conjugated to the QD-encoded beads was designed and tested in biological assays to detect target DNA sequences. Target DNA molecules to be quantified were labeled with a fluorescent dye (Cascade Blue). The dye was chosen to have an absorption band that allows its excitation simultaneously with the codes within the QD-beads, while having emission distinguishable from the coding signal (i.e., no overlap between the dye and bead emissions). Assays were performed at the single bead level, yielding both the DNA identity (based on the QD barcode) as

well as its abundance (based on Cascade Blue emission). The DNA sequence was identified by the coding signal (i.e., optical code of the bead defined by the spectral definition of the emission and the relative intensity of each embedded QD color). Signal from the dye attached to the DNA target accounted for the amount of the target material present in the assayed sample.

3.7. Biomaterials applications of QDs

DNA-mediated assembly of CdS quantum dots into carefully designed layered arrays attached to electrode surfaces has been demonstrated, followed by generation of photoinduced current by the layered arrays in the presence of a sacrificial electron donor (Willner et al., 2001). Microemulsion-grown CdS nanoparticles capped with cystamine/thioethanesulfonate were derivatized with an estimated 20-24 thiolated oligonucleotides per nanoparticle. These DNA-modified QDs were tethered by hybridization to a gold electrode surface previously derivatized with thiolated 13-mer capture DNA, forming a first layer of DNA-QDs. Subsequent layers (up to four total) were built up by hybridization using additional oligo-DNA modified nanoparticles; the layering process could be observed using quartz crystal microgravimetry, absorbance and fluorescence methods. Current flow was observed upon illumination, and photocurrent amplitude correlated closely with absorbance spectra of the arrays. The photocurrent could be switched on and off by cycled illumination. Photocurrent generation likely involved the photoejection of conduction-band electrons of CdS particles in contact with or within tunneling distance of the electrode. Improved photocurrent generation (approximately 2-fold) could be obtained by treating arrays with 5×10^{-6} M $[Ru(NH_3)_6]^{3+}$, which presumably electrostatically interacts with the DNA network. Multiple bound ruthenium complexes may form a conduit for delivery of electrons to the electrode. Finally, a unique assay for DNA was shown, in which specific hybridization of an oligonucleotide (10^{-9} M lower limit) was detected by changes in photocurrent in a two-layer CdS-DNA cross-linked array.

4. Advantages and Limitations

Colloidal semiconductor quantum dots have a number of important advantages over conventional organic fluorophores. The QD absorption spectrum extends into the UV, regardless of size, making it possible to excite multiple sized (colored) particles with one excitation wavelength; organic fluorophores, on the other hand, often have discrete, widely spaced, singlet transitions. In addition, QDs have large extinction coefficients, which translate to absorption cross-sections on the order of 10^{-15} cm^2. By contrast, many organic dyes have absorption cross-sections nearly an order of magnitude smaller than 10^{-16} cm^2. These properties, as well as the color variation made possible by simply varying the physical size of the particle (as opposed to synthesizing new analogs or

derivatives of conventional organic dyes) represent major advantages of QDs, especially in light of potential multiplexing applications.

With respect to their emission, the quantum yields (QYs) of QDs can be comparable to those of organic dyes with values close to 30%. Although they are not as bright as some of the best organic laser dyes such as Rhodamine 6G (QY ~ 95%), they outperform organic fluorophores in two ways. First, the colloidal QDs have narrow (~30-40 nm full width at half maximum) and symmetric emission spectra. Organic dyes, on the other hand, often have broad, asymmetric spectra with a distinct phonon progression to the red. This is a limiting factor in the case of multiplexing applications due to undesirable spectral cross talk among different detector channels. Second, organic dyes suffer from rapid irreversible photodegradation effects, a process often referred to as "photobleaching". While the causes of this effect are not completely understood, photooxidation and other types of degradative photochemistry effectively destroy dye molecules or quench their emission (Eggeling et al., 1999). Semiconductor QDs are much less susceptible to photobleaching since they are made of inorganic materials. This dramatic difference in photostability has been observed at the ensemble level and at the single particle level, where a single CdSe QD has been observed to emit 10^8 photons with no evidence of photobleaching. That value decreases to ~ 10^5-10^6 photons for organic dyes (Kuno et al., 2001).

Fluorescence resonance energy transfer (FRET), a phenomenon that involves nonradiative transfer of excited state energy from a donor to an acceptor, has an efficiency that depends on the degree of overlap between the donor emission spectrum and the absorption spectrum of the acceptor. Early experiments reported efficient Förster energy transfer between neighboring closely packed colloidal QDs of different sizes (Kagan et al., 1996). The tunable and narrow PL spectra of QDs make them potentially very suitable for biosensing applications based on energy transfer, where dye-labeled receptors conjugated to colloidal QDs can report binding events. Experiments demonstrating that QD luminescence can be quenched by surface-bound acceptor dyes in QD-protein conjugates in solution and in solid-phase formats have been described (Willard et al., 2001; Tran et al., 2002).

Substantial difficulties are associated with making QDs water-soluble and derivatizable. No consistent protocol for achieving QD water-compatibility has been devised that can be applied to a wide range of QD materials. As discussed above, a number of methods exist for coating CdSe, CdSe-ZnS, CdS, or CdTe nanocrystals. Most published works to date have focused on the use of CdSe-ZnS QDs, with a few exceptions where CdS, CdSe-CdS, or CdTe QDs have been used (Mahtab et al. 1996; Bruchez et al., 1998; Mamedova et al., 2001). However, at this time, materials with cores made of materials other than CdSe tend to have low quantum yields and poor resistance to degradation in aqueous environments.

In our experience, although CdSe-ZnS QDs capped with DHLA are relatively stable and easy to handle, they have a quite limited functional pH range. For instance, DHLA-capped QDs are stable in basic solutions at pH > 7, but aggregation, often accompanied by loss of luminescence, takes place even in "mildly" acid solutions. Surface functionalization using a porous silica shell is reported to provide stable water-compatible QDs, but the coating process is tedious and tends to result in small amounts of material having a low quantum yield. QD conjugation to proteins has often been carried out using EDC condensation. However, even though this type of chemistry is well established for labeling biomacromolecules with organic dyes, conjugation to QDs can produce irreversible aggregation that may be either immediate or can develop with time (Mattoussi et al., 2000). Non-covalent, electrostatically driven QD-bioconjugate self-assembly can ameliorate aggregation problems in some cases, but it requires the use of surface-charged nanoparticles and oppositely charged proteins with the appropriate biological activity.

Other potential problems that may complicate analysis and understanding of experiments using QD-conjugates derive from the size dependence of their optical properties (e.g., emission) and from the stoichiometry of the QD-biomolecule complexes. Thus, particles emitting further in the red are larger and thus have different diffusion characteristics than smaller ones. This may, for example, complicate experiments where diffusion and dynamics of particle movement within a cell are important. In addition, QDs conjugated with multiple protein receptors or DNA oligomers per dot will have different mobility and likely experience different avidity effects than 1:1 QD:biomolecule conjugates. This may limit their usefulness in some applications.

5. Potential for Use of Quantum Dots in Bio-related Applications

Semiconductor nanocrystals continue to be viewed as potentially extremely useful materials in the realm of biotechnology (Niemeyer, 2001), and the work performed so far in a number of laboratories reaffirms this expectation. Nonetheless, although great strides have been made in the short period of time since the introduction of QDs in biocompatible forms, the state of our knowledge, both in terms of basic science and of nanoengineering technology, is far from mature. Substantial opportunities will exist for new contributions in this dynamic area for the foreseeable future, particularly in the areas of DNA and protein microarray technology, fluorescence-based imaging, and high-throughput drug candidate screening.

The major near-term focus will likely be on uses of QD bioconjugates as photostable substitutes for organic fluorophores as well as in multi-color barcode applications. In the former case, expanded usefulness will come when functional problems related to nanocrystal surface chemistry are solved. Remaining

obstacles in this area include surface oxidation, long-term stability in physiological environments, passivation methods needed to reduce non-specific interactions, and potential toxicity issues related to *in vivo* use. Further expansion of usefulness would also accrue from development of robust biocompatible near IR and IR-emitting materials. Linked to the these obstacles is the fact that there currently exists no acceptable way to mass-produce biocompatible QDs and QD conjugates inexpensively, a situation which will surely hinder wider usage of these materials in new applications until it is overcome.

In the case of potential use of QDs and mixtures of QDs as molecular barcode elements, most likely encapsulated within polymer spheres, an obvious advantage is the inherent multiplex nature of the materials due to their nearly infinite flexibility with respect to excitation wavelengths. This flexibility should translate into simpler and less expensive optical platforms used in barcode applications. In fact, QDs embedded into microbeads have already been tested in this scenario (Han et al., 2001). It should be noted, however, that organic dye-based microsphere technology is quite advanced and may be expected to present considerable competition for analogous QD-based applications. A case in point is the high throughput flow cytometer and associated dye-labeled microsphere reagents commercialized by Luminex (Austin, TX). The system is capable of identifying 100 or more different bead types by the dye ratio contained in each. The amount of fluorescent analyte or antibody bound to each bead is simultaneously measured. In this manner very rapid multiple homogeneous assays can be performed (Kettman et al., 1998; Vignali, 2000; Iannone et al., 2001, Ye et al., 2001).

Although semiconductor nanocrystals as replacements for organic fluorophores will likely account for the bulk of their near-term uses, exploitation of some of their other unique properties in bio-related scenarios is possible. As an example, experiments involving QD bioconjugates binding to neural receptors point to the possibility of utilizing the optoelectronic properties of nanocrystals in less obvious, more sophisticated ways (Winter et al., 2001). Finally, understanding the behavior of the nanocrystals and their bioconjugates at the single particle level will contribute to as yet undiscovered applications. We anticipate that fuller understanding of single-dot phenomena such as intermittent blinking, spectral shifts, effects of crystal lattice defects and surface traps, etc., will lead to development of new types of nanosensors and provide materials for additional bio-related applications.

6. Acknowledgements

We thank Professor M.G. Bawendi from MIT and Drs. B.L. Justus and F.S. Ligler from NRL for the fruitful discussions and useful suggestions. Financial support from the Office of the Naval Research (ONR, Dr. K. Ward), grants # N0001499WX30470, # N0001400WX20094 and # N0001401WX20854, is highly appreciated. The views, opinions, and/or findings described in this report are those of the authors and should not be construed as official Department of the Navy positions, policies or decisions.

7. References

Alivisatos, A.P., 1996, Science 271, 933.

Artmeyev, M.V., S.V. Gaponenko, I.N. Germanenko and A.M. Kapitonov, 1995, Chem. Phys. Lett. 243, 450.

Borrelli, N.F., D.W. Hall, H.J. Holland and D.W. Smith, 1987, J. Appl. Phys. 61, 5399.

Bowen Katari, J.E., V.L. Colvin and A.P. Alivisatos, 1994, J. Phys. Chem. 98, 4109.

Bruchez, M., Jr., M. Moronne, P. Gin, S. Weiss and A.P. Alivisatos, 1998, Science 281, 2013.

Chamarro, M., C. Gourdon, P. Lavallard, O. Lublinskaya and A.I. Ekimov, 1995, Nuovo. Cim. Soc. Ital. Fis. D 17, 1407.

Chamarro, M., C. Gourdon, P. Lavallard, O. Lublinskaya and A.I. Ekimov, 1996, Phys. Rev. B 53, 1336.

Chan, W.C.W. and S. Nie, 1998, Science 281, 2016.

Chepic, D.I., Al.L.Efros, A.I. Ekimov, M.G. Vanov, V.A. Kharchenko, I.A. Kudriavtsev and T.V. Yazeva, 1990, J. Luminesc. 47, 113.

Chestnoy, N., R. Hull and L.E. Brus, 1986, J. Chem. Phys. 85, 2237.

Colvin, V.L., M.C. Schlamp and A.P. Alivisatos, 1994, Nature 370, 354.

Cook, R.J. and H.J. Kimble, 1985, Phys. Rev. Lett. 54, 1023.

Dabbousi, B.O., M.G. Bawendi, O. Onitsuka and M.F. Rubner, 1995, Appl. Phys. Lett. 66, 1316.

Dabbousi, B.O., J. RodriguezViejo, F.V. Mikulec, J.R. Heine, H. Mattoussi, R. Ober, K.F. Jensen and M.G. Bawendi, 1997, J. Phys. Chem. B 101, 9463.

Dahan, M., T. Laurence, F. Pinaud, D.S. Chemla, A.P. Alivisatos, M. Sauer and S. Weiss, 2001, Optics Lett. 26, 825.

Efros, A.L., M. Rosen, M. Kuno, M. Nirmal, D.J. Norris and M.G. Bawendi, 1996, Phys. Rev. B54, 4843.

Efros, A.L. and M. Rosen, 1997, Phys. Rev. Lett. 78, 1110.

Efros, A.L. and M. Rosen M., 2000, Ann. Rev. Mater. Sci. 30, 475.

Eggeling, C., J. Widengren, R. Rigler and C.A.M. Seidel, 1999, In Applied Fluorescence in Chemistry, Biology and Medicine, W. Rettig, B. Strehmel, S. Schrader, H. Seifert, Eds., Springer, Berlin, pp. 193.

Ekimov, A.I., A.A. Onuschenko and V.A. Tsekhomskii, 1980, Fiz. Khim. Stekla 6, 511.

Ekimov, A.I. and A.A. Onuschenko, 1981, JETP Lett. 34, 345.

Ekimov, A.I. and A.A. Onuschenko, 1982, Sov. Phys. Semicond. 16, 775.

Ekimov, A.I. and A.A. Onuschenko, 1984, JETP Lett. 40, 337.

Ekimov, A.I., A.A. Onuschenko, A.G. Pluhkin and A.L. Efros, 1985, JETP Lett. 88, 1490.

Ekimov, A.I., A.L Efros and A.A. Onuschenko, 1985, Sol. Stat. Comm. 56, 921.

Ekimov, A.I., F.Hache, M.C. Schanneklein, D. Ricard, C. Flytzanis, I.A. Kudryavtsev, T.V. Yazeva, A.V. Rodina and A.L. Efros, 1993, J. Opt. Soc. Am. B-Opt. Phys. 10, 100.

Ekimov, A.I., 1996, J. Luminesc. 70, 1.

Gaponenko, S.V., U. Woggon, M. Saleh, W. Langbein, A. Uhrig, M. Muller and C. Klingshirn, 1993, J. Opt. Soc. Am. B-Opt. Phys. 10, 1947.

Gaponenko, S.V., 1998, Optical Properties of Semiconductor Nanocrystals, Cambridge University Press, Cambridge, 260 pp.

Gaponik, N.P., D.V. Talapin, A.L. Rogach, A. Eychmuller, 2000, J. Mat. Chem. 10, 2163.

Gearheart, L., K.K. Caswell and C.J. Murphy, 2001, J. Biomed. Optics, 6, 111.

Goldman, E.R., E.D. Balighian, M.K. Kuno, S. Labrenz, P.T. Tran, G.P. Anderson, J.M. Mauro and H. Mattoussi, 2002, Phys. Stat. Sol., in press.

Goldman, E.R., G.P. Anderson, P.T. Tran, H. Mattoussi, P.T. Charles and J.M. Mauro, 2002, Anal. Chem., in press.

Goldman, E.R., H. Mattoussi, P.T. Tran, G.P. Anderson and J.M. Mauro, 2001, In Semiconductor Quantum Dots, Ed, S. Fafard, D. Huffaker, R. Leon and R. Noetzel, Mat. Res. Soc. Pro., Pittsburgh, 642, J2.8.1.

Greenham, N.C., X.G. Peng. and A.P. Alivisatos, 1996, Phys. Rev. B54, 17628.

Gurevich, S.A., A.I. Ekimov, I.A. Kudryavtsev, A.V. Osinskii, V.I. Skopina and D.I. Chepik, 1992, Sov. Phys. Semicond. 26, 57.

Hall, D.W. and Borrelli N.F., 1988, J. Opt. Soc. Am. B-Opt. Phys. 5,1650.

Han, M., X. Gao, J.Z. Su and S. Nie, 2001, Nature Biotech.19, 631.

Henglein, A., 1982, Ber. Bunsen Phys. Chem. 86, 301.

Hermanson, G.T., 1996, Bioconjugate Techniques, Academic Press: London.

Herron, N, Y. Wang, M.M. Edd, G.D. Stucky, D.E. Cox, K. Moller and T. Bein, 1989, J. Am. Chem. Soc. 111, 530.

Hines, M.A. and P. Gnyot-Sionnest, 1996, J. Phys. Chem. B 100, 468.

Hines, M.A. and P. Guyot-Sionnest, 1998, J. Phys. Chem. B 102, 3655.

Hodes, G., A. Albuyaron, F. Decker and P. Motisuke, 1987, Phys. Rev. B 36, 4215.

Hu, J.T., L.S. Li, W.D. Yang, L. Manna, L.W. Wang and A.P. Alivisatos, 2001, Science 292, 2060.

Iannone, M.A., T.G. Consler, K.H. Pearce, J.B. Stimmel, D.J. Parks and J.G. Gray, 2001, Cytometry 44, 326.
Kagan C.R., C.B. Murray and M.G. Bawendi, 1996, Phys. Rev. B 54, 8633.
Kettman, J.R., T.Davies, D. Chandler, K.G. Oliver and R.J. Fulton, 1998, Cytometry 33, 234.
Kortan, A.R., R. Hull, R.L. Opila, M.G. Bawendi, M.L. Steigerwald, P.J. Carrolla and L.E. Brus, 1990, J. Am. Chem. Soc. 112, 1327.
Kotov, N.A., K. Putyera, J.H. Fendler, E. Tombacz and I. Dekany, 1993, Coll. Surf. A-Phys. Eng. Aspects 71, 317.
Kotov, N.A., F.C. Meldrum, C. Wu and J.H. Fendler, 1994, J. Phys. Chem. 98, 2735.
Kuno, M., J.K. Lee, B.O. Dabbousi, F.V. Mikulec and M.G. Bawendi, 1997, J. Chem. Phys. 106, 9869.
Kuno, M., D.P. Fromm, H.F. Hamann, A. Gallagher and D.J. Nesbitt, 2001, J. Chem. Phys. 115, 1028
Liu, L.C. and S.H. Risbud, 1990, J. Appl. Phys. 68, 28.
Liu, L.C., M.J. Kim, S.H. Risbud and R.W. Carpenter, 1991, Philosoph. Mag. B 63, 769.
Lobenhofer E.K., P.R. Bushel, C.A. Afshari and H.K. Hamadeh, 2001, Env. Health Pers. 109, 881.
Mahtab, R., J.P. Rogers, C.P. Singleton and C.J. Murphy, 1996, J. Am. Chem. Soc., 118, 7028.
Mamedova, N.N., N.A. Kotov, A.L. Rogach and J. Studer, 2001, Nano Lett. 1, 281.
Mathieu, H., T. Richard, J. Allegre, P. Lefebvre and G. Arnaud, 1995, J. Appl. Phys. 77, 287.
Mattoussi, H., A.W. Cumming, C.B. Murray, M.G. Bawendi, and R. Ober, 1998-II, Phys. Rev. B 58, 7850.
Mattoussi, H., L.H. Radzilowski, B.O. Dabbousi, E.L. Thomas, M.G. Bawendi and M.F. Rubner, 1998, J. Appl. Phys. 83, 7965.
Mattoussi, H., J.M. Mauro, E.R. Goldman, G.P. Anderson, V.C. Sundar, F.V. Mikulec and M.G. Bawendi, 2000, J. Am. Chem. Soc. 122, 12142.
Mattoussi, H., J.M. Mauro, E.R. Goldman, R.M. Green, G.P. Anderson, V.C. Sundar and M.G. Bawendi, 2001, Phys. Stat. Sol. 224, 277.
Meyer, M., C. Wallberg, K. Kurihara and J.H. Fendler, 1984, J. Chem. Soc. Chem. Commun. 90, 90.
Mikulec, F.V., 1999, Ph.D. Dissertation, Massachusetts Institute of Technology.
Minti, H., M. Eyal, R. Reisfeld and G. Berkovic, 1991, Chem. Phys. Lett. 183, 277.
Misawa, K., H. Yao, T. Hayashi and T. Kobayashi, 1991, Chem. Phys. Lett. 183, 113.
Misawa, K., H. Yao, T. Hayashi and T. Kobayashi, 1991, J. Chem. Phys. 94, 4131.
Mitchell, G.P., C.A. Mirkin and R.L. Letsinger, 1999, J. Am. Chem. Soc. 121, 8122.

Murray, C.B., S. Sun, W. Gaschler, H. Doyle, T.A. Betley and C.R. Kagan, 2001, IBM J. Res. Dev. 45, 47.
Murray, C.B., C.R. Kagan and M.G. Bawendi, 2000, Ann. Rev. Mater. Sci. 30, 545.
Murray, C.B., D.J. Norris and M.G. Bawendi, 1993, J. Am. Chem. Soc. 115, 8706.
Niemeyer, C.M., 2001, Angew. Chem. Int. Ed. 40, 4218.
Nirmal, M., D.J. Norris, M. Kuno, M.G. Bawendi, A.L. Efros and M. Rosen, 1995, Phys. Rev. Lett. 75, 3728.
Nirmal, M., B.O. Dabbousi, M.G. Bawendi, J.J. Macklin, J.K. Trautman, T.D. Harris and L.E. Brus, 1996, Nature 383, 802.
Nogami, M., K. Nagasaka and M. Takata, 1990, J. Non-Cryst. Sol. 122, 101.
Norris, D.J., N. Yao, F.T. Charnock and T.A. Kennedy, 2001, Nano Lett. 1, 3.
Ochoa, R.O., C. Colajacomo, E.J. Witkowski, J.H. Simmons and B.G. Potter, 1996, Sol. Stat. Comm. 98, 717.
Pathak, S., S.K. Choi, N. Arnheim and M.E. Thompson, 2001, J. Am. Chem. Soc. 123, 4103.
Peng, X., M.C. Schlamp, A.V. Kadavanich, U. Banin and A.P. Alivisatos, 1997, J. Am. Chem. Soc. 119, 7019.
Peng, X.G., L. Manna, W.D. Yang, J. Wickham, E. Scher, A. Kadavanich and A.P. Alivisatos, 2000, Nature 404, 59.
Peng, Z.A. and X.G. Peng, 2001, J. Am. Chem. Soc. 123, 183.
Peng, Z.A. and X.G. Peng, 2001, J. Am. Chem. Soc. 123, 1389.
Persans, P.D., A. Tu, Y.I. Wu and M. Lewis, 1989, J. Opt. Soc. Am. B-Opt. Phys. 6, 818.
Pileni M.P., L. Motte and C. Petit, 1992, Chem. Mater. 4, 338.
Potter, B.G. and J.H. Simmons, 1988, Phys. Rev. B 37, 10838.
Potter, B.G. and J.H. Simmons, 1988, J. Appl. Phys. 68, 1218.
Qu, L., Z.A. Peng and X.G. Peng, 2001, Nano Lett. 1, 333.
Rodriguez-Viejo, J., H. Mattoussi, J.R. Heine, M.K. Kuno, J. Michel, M.G. Bawendi, and K.F. Jensen, 2000, J. Appl. Phys. 87, 8526.
Roederer, M., S. DeRosa, R. Gerstein, M. Anderson, M. Bigos, R. Stovel, T. Nozaki, D. Parks, L. Herzenberg and L. Herzenberg, 1997, Cytometry 29, 328.
Rogach, A.L., L. Katsikas, A. Kornowski, D. Su, A. Eychmuller and H. Weller, 1997, Ber. Bunsen. Phys. Chem. 101, 1668.
Rossetti, R., S. Nakahara and L.E. Brus, 1983, J. Chem. Phys. 79, 1086.
Rossetti, R., J.E. Ellison, J.M. Gibson and L.E. Brus, 1984, J. Chem. Phys. 80, 4464.
Schlamp, M.C., X.G. Peng and A.P. Alivisatos, 1997, J. Appl. Phys. 82, 5837.
Schröck, E., S. du Manoir, T. Veldman, B. Schoell, J. Wienberg, M.A. Ferguson-Smith, Y. Ning, D.H. Ledbetter, I. Bar-Am, D. Soenksen, Y. Garini and T. Ried, 1996, Science, 273, 494.
Spanhel L., E. Arpac and H. Schmidt, 1992, J. Non-Crys. Sol. 147, 657.
Sondi, I., O. Siiman, S. Koester and E. Matijevic, 2000, Langmuir 16, 3107.

Steigerwald, M.L., A.P. Alivisatos, J.M. Gibson, T.D. Harris, R. Kortan, A.J. Muller, A.M. Thayer, T.M. Duncan, D.C. Douglass and L.E. Brus, 1988, J. Am. Chem. Soc. 110, 3046.

Steigerwald, M.L. and L.E. Brus, 1989, Ann. Rev. Mat. Sci. 19, 471.

Sun, B., W. Xie, G. Yi, D. Chen, Y. Zhou, and J. Cheng, 2001, J. Immunol. Meth., 249, 85.

Tedeschi, C.; F. Caruso, H. Möhwald and S. Kirstein, 2000, J. Am. Chem. Soc. 122, 5841.

Tran, P.T., E.R. Goldman, H. Mattoussi, G.P. Anderson and J.M. Mauro, 2001, Proc. SPIE 4258, 1.

Tran, P.T., E.R. Goldman, G.P. Anderson, J.M. Mauro and H. Mattoussi, 2002, Phys. Stat. Sol., In Press.

Trindade T., P. O'Brien, N.L. Pickett, 2001, Chem. Mat. 13, 3843.

Vignali, D.A.A., 2000, J. Immunol. Methods 243, 243.

Wang, Y, N. Herron, W. Mahler and A. Suna, 1989, J. Opt. Soc. Am B-Opt. Phys. 6, 808.

Weller, H, H.M. Schmidt, U.Koch, A. Fojtik, S. Baral, A. Henglein, W. Kunath, and K. Weiss, 1986, Chem. Phys. Lett. 124, 557.

Willard, D.M., L.L. Carillo, J. Jung and A.Van Orden, 2001, Nano Lett. 1, 469.

Willner, I., F. Patolsky and J. Wasserman, 2001, Ang. Chem. Intl. Ed. 40, 1861.

Winter, J.O., T.Y. Liu, B.A. Korgel and C.E. Schmidt, 2001, Adv. Mater. 13, 1673.

Woggon, U., S.V. Bogdanov, O. Wind, K.-H., Schlaad, H. Pier, C. Klingshirn, P. Chatziagorastou and H.P. Fritz, 1993, Phys. Rev. B48, 11979.

Woggon, U., 1997, Optical Properties of Semiconductor Quantum Dots, Springer-Verlag, Berlin, 251 pp.

Ye, F., M.S. Li, J.D. Taylor, Q. Nguyen, H.M. Colton, W.M. Casey, M. Wagner, M.P. Weiner and J. Chen, 2001, Hum. Mutat. 17, 305.

Yoffe, A.D., 1993, Adv. Physics, 42, 173.

Yoffe, A.D., 2001, Adv. in Physics 50, 1.

Zhao, X.S., J. Schroeder, P.D. Persans and T.G. Bilodeau, 1991, Phys. Rev. B 43, 12580.